

## On the robustness of the topological derivative for Helmholtz problems and applications\*

by

Günter Leugering<sup>1</sup>, Antonio André Novotny<sup>2</sup> and Jan Sokolowski<sup>3</sup>

<sup>1</sup>FAU Senior Fellow of Applied Mathematics, Department of Data Science,  
Friedrich-Alexander-Universität Erlangen-Nürnberg (FAU),  
Cauerstrasse 11, 91058 Erlangen, Germany

<sup>2</sup>Laboratório Nacional de Computação Científica, LNCC/MCTI,  
Coordenação de Métodos Matemáticos e Computacionais,  
Av. Getúlio Vargas 333, 25651-075 Petrópolis – RJ, Brazil

<sup>3</sup>Systems Research Institute, Polish Academy of Sciences,  
Newelska 6, 01-447 Warszawa, Poland

**Abstract:** We consider Helmholtz problems in two and three dimensions. The topological sensitivity of a given cost function  $J(u_\epsilon)$  with respect to a small hole  $B_\epsilon$  around a given point  $x_0 \in B_\epsilon \subset \Omega$  depends on various parameters, like the frequency  $k$  chosen or certain material parameters or even the shape parameters of the hole  $B_\epsilon$ . These parameters are either deliberately chosen in a certain range, as, e.g., the frequencies, or are known only up to some bounds. The problem arises as to whether one can obtain a uniform design using the topological gradient. We show that for 2-d and 3-d Helmholtz problems such a robust design is achievable.

**Keywords:** topological derivative, shape optimization, inverse problems, Helmholtz problem, numerical methods, complex variables

### 1. Introduction

#### 1.1. General framework of compound asymptotics method for elliptic boundary value problems

An efficient method of shape and topology optimization is called the topological derivative method, see Novotny and Sokolowski (2013, 2020). In contrast to the

---

\*Submitted: March 2022; Accepted: June 2022.

boundary variations technique, the shape gradient obtained by the topological derivative method allows for the topology changes of the domain of integration.

The topological derivatives (TD) are obtained using the asymptotic methods for singular perturbations of geometrical domains for elliptic PDE's. In practice, the continuous TD is used for the associated discrete problems. Namely, the approximation of solutions to the PDEs by the finite element (FE) method is employed in numerical methods of shape and topology optimization. Therefore, the robustness with respect to parameters of formula for TDs is required to obtain meaningful numerical results by an application of the TD method in shape optimization or in inverse problems. Such results are derived here for the representative case of the Helmholtz boundary value problems. The method used is general and could be repeated for the elliptic boundary value problems. The numerical results confirm the robustness of TD for a model problem useful for applications.

The technique, used for approximation of solutions to boundary value problems with small size geometrical singularities, employs the so-called *interior* and *exterior* asymptotic expansions in two regions of the geometrical domain. The asymptotic expansions depend on the small parameter, which measures the size of the defect. Let us recall that the size of the defect in the form of a hole is measured by its Newtonian capacity. We refer for the details to the monograph by Arlen M. Il'in (1992).

## 1.2. The topological derivative method in shape optimization

The topological derivative has been specifically conceived to provide a precise information on the sensitivity of a given shape functional with respect to topological domain perturbations. It appears in the first term of the asymptotic expansion of the shape functional with respect to a small parameter measuring the size of the perturbation under consideration, typically a hole, an inclusion, a source-term, or a crack.

The origin of the topological derivative method in optimal design can be dated to the work by Schumacher (1995) on the optimal location of holes within elastic structures. It is nevertheless worth mentioning the prior related mathematical developments on the asymptotic behaviour of solutions to singularly perturbed boundary value problems and on the notions of polarization and capacity matrices. These objects are essential ingredients in the formulation of topological derivatives. The first mathematical justifications for topological derivatives in the framework of partial differential equations are due to Sokolowski and Żochowski (1999) and Garreau, Guillaume and Masmoudi (2001), in the context of the Poisson equation and the Navier system for Neumann and Dirichlet holes.

In the last decade, the topological sensitivity analysis has become a rich and fascinating research field that combines the modern theory of calculus of vari-

ations, partial differential equations, differential geometry, numerical analysis, physics, engineering and computational mechanics. The field grew up rapidly to develop many extensions and address a variety of physical and industrial problems. The topological derivative method has applications in shape and topology optimization, geometrical inverse problems, image processing, multi-scale material design and mechanical modelling, including damage and fracture evolution phenomena. See, for instance, the books by Novotny and Sokołowski (2013, 2020), and by Novotny, Sokołowski and Źochowski (2019).

In this paper, we consider a class of shape/topology optimization problems governed by the Helmholtz equation in two and three spatial dimensions. The topological derivatives, associated with the nucleation of inclusions as well as holes endowed with homogeneous Dirichlet or Neumann boundary conditions, are presented. In particular, we show that the topological derivative is robust with respect to variations in the working frequency and system parameters. Finally, we present some applications of the topological derivative method in the context of imaging of small scatters from boundary measurements.

## 2. Shape optimization for Helmholtz boundary value problems

The problem, which we want to consider in this paper is motivated by applications in acoustic and electromagnetic scattering, in which, according to a given cost or merit function, the topology of the domain has to be optimized, in particular using topological sensitivities. More specifically, given a domain  $\Omega \subset \mathbf{R}^d$   $d = 2, 3$ , we consider solutions  $u(x, t)$ ,  $(x, t) \in \Omega \times [0, T]$  of the wave equation (Assous, Ciarlet and Labrunie, 2018)

$$\left\{ \begin{array}{l} \frac{\partial^2}{\partial t^2} u = \Delta u, \quad \text{in } \Omega \times (0, T) \\ u = 0 \quad \text{on } \Gamma_0 \times (0, T) \\ \frac{\partial}{\partial n} u = \gamma \frac{\partial}{\partial t} u + h \quad \text{on } \Gamma_1 \times (0, T) \\ u(\cdot, 0) = u_0, \quad \frac{\partial}{\partial t} u(\cdot, 0) = u_1 \quad \text{in } \Omega, \end{array} \right. \quad (2.1)$$

where  $\partial\Omega = \Gamma_0 \cup \Gamma_1$ . Upon denoting  $u_\Omega := u$  one is interested in evaluating a cost-function  $J(\Omega) := J(u_\Omega)$ . One then poses the shape- or topology-optimization problem

$$J(\Omega^*) := \inf_{\Omega} J(\Omega), \quad (2.2)$$

where  $\Omega$  may be chosen in a given class of sets. See Sokolowski and Zolésio (1992), Henrot and Pierre (2005) as standard references in shape optimization. While the classical 'speed-method' in shape optimization, where the shapes undergo a flow driven by 'shape-gradients', will not allow for topology changes,

the notion of 'topological gradients' aims precisely at 'digging a hole' into the domain, thereby changing the topology locally, which gives rise to further inspection, e.g., using the speed-method.

To be more precise, let us introduce an open subset  $B \subset \mathbf{R}^d$  such that  $0 \in B$  and a point  $x_0 \in \Omega$  such that  $B_\epsilon(x_0) := x_0 + \epsilon B \subset \Omega$ ,  $\forall \epsilon \in [0, \epsilon_0)$ . Then one introduces the topological derivative as follows

$$\mathcal{T}(x_0) := \lim_{t \rightarrow 0^+} \frac{J(\Omega \setminus \overline{B_\epsilon(x_0)}) - J(\Omega)}{|B_\epsilon(x_0)|}. \quad (2.3)$$

If  $\mathcal{T}(x_0) < 0$ , then a topology change at  $x_0$  will decrease the cost function, and, consequently, a shape-step may be used or the procedure is repeated in the neighborhood of  $x_0$  etc. This procedure has been developed in Sokolowski and Żochowski (1999a,b, 2001). Topological sensitivities have become a major tool in shape and topology optimization. See Amstutz & Novotny (2010), Mas-moudi, Pommier and Samet (2005), Allaire, Jouve and Toader (2004), mostly for the analysis of classical material and numerical implementation, and Bonnet and Guzina (2004), Guzina and Chichikev (2007), Hintermüller (2005) and others for applications, e.g., in mechanical engineering, geophysics and medical imaging. The number of articles has increased tremendously, so that seeking a complete list of references is inordinate. See the special issue on the topological derivative method and its applications in computational engineering, recently published in the *Engineering Computations Journal* (Novotny, Giusti and Amstutz, 2022), covering various topics ranging from new theoretical developments (Amstutz, 2022; Baumann and Sturm, 2022; and Delfour, 2022) to applications in structural and fluid dynamics topology optimization (Kliewe, Laurain and Schmidt, 2022; Romero, 2022; and Santos and Lopes, 2022), geometrical inverse problems (Bonnet, 2022; Canelas and Roche, 2022; Fernandez and Prakash, 2022; Le Louër and Rapún, 2022a,b), synthesis and optimal design of metamaterials (Ferrer and Giusti, 2022; Yera et al., 2022), fracture mechanics modelling (Xavier and Van Goethem, 2022), up to industrial applications (Rakotondrainibe, Allaire and Orval, 2022) and experimental validation of the topological derivative method (Barros et al., 2022).

Among the problems of mathematical physics that have been investigated so far are Helmholtz-type problems in 2-d and 3-d, where we would like to mention in particular the work by Samet et al. (2003). Even though the time dependent problems like (2.1) have been considered recently, many questions remain open. In mechanical engineering one is typically interested in the behavior of the system for a particular range of frequencies rather than for the time-evolution. Therefore, one introduces the time-harmonics as follows

$$u(x, t) = e^{ikt}u(x), \quad h(x, t) = e^{ikt}h(x). \quad (2.4)$$

Using (2.4) in (2.1) we obtain a Helmholtz problem of the form

$$\begin{cases} \Delta u + k^2 u = 0 & \text{in } \Omega \\ u = 0 & \text{on } \Gamma_0 \\ \frac{\partial}{\partial n} u - \gamma i k u = h & \text{on } \Gamma_1, \end{cases} \quad (2.5)$$

where  $u$  is now a complex quantity.

Topological derivatives for problems like (2.5) have been investigated, e.g., in Samet, Amstutz and Masmoudi (2003), where in the 2-d case the set  $\Gamma_0$  is assumed to have positive measure, whereas in the 3-d case Neumann conditions hold throughout  $\Gamma$ . Quite obviously, the topological derivative developed there depends on the frequency parameter  $k$  chosen, and thus the topology may depend on the frequency. This is certainly undesirable, as one typically has to deal with a whole frequency range  $I := [k_0, k_1]$ . Therefore, the natural question is as to whether an 'average-design' can be derived from the knowledge of  $\mathcal{T}(x_0; k)$ . A similar question arises when one has to account for uncertainties in some other physical parameters of the problem. Finally, the shape of the bona-fide topology change may play a role in the design. A first approach in dealing with robustness problems regarding topological sensitivities has been presented by Hlavacek, Novotny, Sokolowski and Zochowski (2009). There, the authors introduce a worst-case design and a so-called maximum range design. They develop the concept in the context of 2-d and 3-d elasticity, where the robustness is investigated with respect to changes in the material parameters, only. In this paper we focus on 2-d and 3-d Helmholtz problems (2.5) and consider robustness with respect to frequencies, data and geometry of the holes or inclusions.

### 3. Notation and basic facts

#### 3.1. The 2-d Helmholtz problem with Dirichlet conditions at the hole

We first consider a 2-d problem with partial Dirichlet conditions (Samet, Amstutz and Masmoudi, 2003). In order to make our analysis transparent, we need to introduce some notation. To this end we denote

$$V_\Omega := \{u \in H^1(\Omega) \mid u = 0 \text{ on } \Gamma_0\}$$

as the reference (complex) 'energy-space'. For the sake of simplicity, we assume that  $\gamma = 1$  in (2.1). We may extend  $k$  to the complex plain  $\mathcal{K} := \{k \in \mathbf{C} \mid \Im(k) \geq 0\}$ , and let  $h \in H_{00}^{\frac{1}{2}}(\Gamma_1)^*$ , the dual of

$$H_{00}^{\frac{1}{2}}(\Gamma_1) := \{\text{tr}|_{\Gamma_1} v, v \in H^1(\Omega), v = 0 \text{ on } \Gamma_0\}.$$

Then we consider the Helmholtz problem (2.5). We are now going to drill a hole into the domain  $\Omega$ . In this first example, for the sake of simplicity, we take a ball  $B_\epsilon(x_0)$  of radius  $\epsilon$  around  $x_0$  and define its complement in  $\Omega$  as  $\Omega_\epsilon := \Omega \setminus \overline{B_\epsilon}$ , whereas the boundary of the hole is denoted by  $\Sigma_\epsilon = \partial B_\epsilon(x_0)$ .

In  $\Omega_\epsilon$  we consider, as in Samet, Austutz and Masmoudi (2003), the perturbed problem

$$\begin{cases} \Delta u_\epsilon + k^2 u_\epsilon = 0 & \text{in } \Omega_\epsilon \\ u_\epsilon = 0 & \text{on } \Gamma_0 \\ \frac{\partial}{\partial n} u_\epsilon - ik u_\epsilon = h & \text{on } \Gamma_1. \end{cases} \quad (3.6)$$

In order to solve (3.6) one introduces the reference space

$$V_\epsilon := \{u \in H^1(\Omega_\epsilon) \mid u = 0 \text{ on } \Gamma_0, u = 0 \text{ on } \Sigma_0\}.$$

However, it is more convenient to introduce the Dirichlet-to-Neumann map or the Steklov-Poincaré operator  $\mathcal{S}_\epsilon^k$  in order to decompose the problem. To this end we introduce  $\Omega_R := \Omega \setminus \overline{B_\epsilon}$  and the annulus  $D_\epsilon := B_R \setminus \overline{B_\epsilon(x_0)}$ . Let now  $u_\epsilon^\psi$  be the solution of the Helmholtz problem on the annulus  $D_\epsilon$

$$\begin{cases} \Delta u_\epsilon^\psi + k^2 u_\epsilon^\psi = 0 & \text{in } D_\epsilon \\ u_\epsilon^\psi = 0 & \text{on } \Sigma_\epsilon \\ u_\epsilon^\psi = 0 & \text{on } \Sigma_R. \end{cases} \quad (3.7)$$

We now define the Dirichlet-to-Neumann map as follows

$$\begin{cases} \mathcal{S} : H^{\frac{1}{2}}(\Sigma_R) \longrightarrow H^{-\frac{1}{2}}(\Sigma_R) \\ \mathcal{S}_\epsilon^k(\psi) := \nabla u_\epsilon^\psi \cdot n|_{\Sigma_R}. \end{cases} \quad (3.8)$$

Equipped with this map, we can solve the original problem on  $\Omega$  via

$$\begin{cases} \Delta u_\epsilon^R + k^2 u_\epsilon^R = 0 & \text{in } \Omega_R \\ u_\epsilon^R = 0 & \text{on } \Gamma_0 \\ \frac{\partial}{\partial n} u_\epsilon^R + \mathcal{S}_\epsilon^k u_\epsilon^R = 0 & \text{on } \Sigma_R \\ \frac{\partial}{\partial n} u_\epsilon^R - ik u_\epsilon^R = h & \text{on } \Gamma_1. \end{cases} \quad (3.9)$$

It is apparent that

$$\begin{cases} u_\epsilon^\psi = u_\epsilon^R & \text{on } \Sigma_R \\ \frac{\partial}{\partial n_{D_\epsilon}} u_\epsilon^\psi + \frac{\partial}{\partial n_{\Omega_R}} u_\epsilon^R = 0 & \text{on } \Sigma_R \end{cases} \quad (3.10)$$

constitute the correct transmission condition in order to conclude  $u_\epsilon = u_\epsilon^R$  on  $D_\epsilon$  and  $u_\epsilon = u_\epsilon^R$  on  $\Omega_R$  such that  $u_\epsilon$  solves (3.6). Again, in connection with problem (3.9) one introduces the space  $V_R := \{u \in H^1(\Omega_R) | u = 0 \text{ on } \Gamma_0\}$ . Then one can derive the following variational form of (3.9). We first define the corresponding sesquilinear form and the 'right-hand-side'

$$\begin{cases} a_\epsilon(u, v; k) := \int_{\Omega_R} \nabla u \cdot \nabla \bar{v} dx - k^2 \int_{\Omega_R} u \bar{v} dx \\ \quad + \int_{\Sigma_R} (\mathcal{S}_\epsilon^k u) \bar{v} d\gamma - ik \int_{\Gamma_1} u \bar{v} d\gamma, \quad \forall u, v \in V_R \end{cases} \quad (3.11)$$

$$\ell(v) := \int_{\Gamma_1} h \bar{v} d\gamma, \quad \forall v \in V_R. \quad (3.12)$$

We are now in the position to state the variational formulation of (3.9)

$$\begin{cases} \text{Find } u_\epsilon^R \in V_R \text{ such that} \\ a_\epsilon(u_\epsilon^R, v; k) = \ell(v), \quad \forall v \in V_R. \end{cases} \quad (3.13)$$

By Proposition 3.1 in Samet, Amstutz and Masmoudi (2003), problem (3.13) admits a unique solution. Notice that the only appearance of the parameter  $\epsilon$  in (3.9) is via the Steklov-Poincaré operator  $\mathcal{S}_\epsilon^k$ . We may then let  $\epsilon = 0$  and consider

$$\begin{cases} \Delta u_0^\psi + k^2 u_0^\psi = 0 \text{ in } B_R(x_0) \\ u_0^\psi = \psi \text{ on } \Sigma_R \end{cases}. \quad (3.14)$$

The associated variational formulation is

$$\begin{cases} \text{Find } u_0^R \in V_R \text{ such that} \\ a_0(u_0^R, v; k) = \ell(v), \quad \forall v \in V_R, \end{cases} \quad (3.15)$$

where  $a_0(u, v; k)$  is obtained by letting  $\epsilon = 0$  in (3.13). The crucial point is that the problem (3.7) can be solved explicitly using Bessel-functions, see Samet, Amstutz and Masmoudi (2003).

**REMARK 3.1** *We need Bessel-functions in order to evaluate the form of topological derivative, required for computations. We assume also that the cost functional  $u \mapsto J(u)$  is defined on the fixed, truncated domain  $\Omega_R$  and it depends on the solution of the variational problem in the truncated domain. In this way we replace the singular geometrical perturbations of  $\Omega$  by the regular perturbations of the Steklov-Poincaré operator in the boundary conditions.*

Following Samet, Amstutz and Masmoudi (2003), we obtain:

$$u_\epsilon^\psi(r, \theta) = \sum_{n \in \mathbf{Z}} \frac{J_n(kr)Y_n(k\epsilon) - J_n(k\epsilon)Y_n(kr)}{J_n(kR)Y_n(k\epsilon) - Y_n(kR)J_n(k\epsilon)} \psi_n e^{in\theta} \tag{3.16}$$

$$\mathcal{S}_\epsilon^k(r, \theta) = k \sum_{n \in \mathbf{Z}} \frac{J'_n(kr)Y_n(k\epsilon) - J_n(k\epsilon)Y'_n(kr)}{J_n(kR)Y_n(k\epsilon) - Y_n(kR)J_n(k\epsilon)} \psi_n e^{in\theta}, \tag{3.17}$$

where  $(r, \theta)$  are the polar coordinates,  $\psi_n$  are the Fourier-coefficients of  $\psi$  and  $J_n, Y_n$  are the Bessel-functions of type I and II, respectively. With  $u_\epsilon^\psi$  and  $\mathcal{S}_\epsilon^k$  we can solve (3.9) and  $u_\epsilon^R, u_\epsilon^s$  satisfy the transmission conditions (3.10). Moreover, the solution to the problem for  $\epsilon = 0$ , together with the Steklov-Poincaré map  $\mathcal{S}_0^k$ , satisfies

$$\begin{cases} u_0^\psi(r, \theta) = \sum_{n \in \mathbf{Z}} \frac{J_n(kr)}{J_n(kR)} \psi_n e^{in\theta} \\ \mathcal{S}_0^k \psi(r, \theta) = k \sum_{n \in \mathbf{Z}} \frac{J'_n(kr)}{J_n(kR)} \psi_n e^{in\theta} \end{cases} \tag{3.18}$$

so that the following crucial asymptotic expansion is valid

$$\|\mathcal{S}_\epsilon^k - \mathcal{S}_0^k - \frac{-1}{\log \epsilon} \delta_S\|_{\mathcal{L}(H^{\frac{1}{2}}(\Sigma_R), H^{-\frac{1}{2}}(\Sigma_R))} = o\left(\frac{-1}{\log \epsilon}\right), \tag{3.19}$$

where  $\delta_S$  is a linear mapping of the form

$$\delta_S \Psi := \frac{1}{RJ_0^2(kR)} \Psi_0$$

and  $\Psi_n$  are the Fourier coefficients of  $\Psi$ .

Hence, the difference of the corresponding forms satisfies

$$\begin{aligned} a_\epsilon(u, v; k) - a_0(u, v; k) &= \int_{\Sigma_R} (\mathcal{S}_\epsilon^k - \mathcal{S}_0^k) u \bar{v} d\gamma \\ &= -\frac{1}{\log \epsilon} \frac{1}{RJ_0^2(kR)} u_0 \int_{\Sigma_R} \bar{v} d\gamma + \dots \\ &= -\frac{1}{\log \epsilon} \frac{2\pi}{R} \frac{u^{\text{mean}} \bar{v}^{\text{mean}}}{J_0(kR)^2} + \dots, \end{aligned}$$

where  $u^{\text{mean}}, v^{\text{mean}}$  denote, respectively, the mean values of  $u$  and  $v$  on  $\Sigma_R$ .

For the sake of simplicity we assume that the shape functional is given by an integral expression, defined on the truncated domain  $\Omega_R$ . Most of the results are valid in the general case. We need also some expansion of the cost with respect to the state in order to define the appropriate adjoint state  $p$  and derive



the simple form of topological derivatives. To this end we introduce a linear mapping  $v \mapsto L_{(u;k)}(v)$  for all directions  $v$ , states  $u$  and frequencies  $k$ .

Let now the cost function admit the expansion

$$J(u + v; k) = J(u; k) + \Re L_{(u;k)}(v) + o(\|v\|_{V_R}), \quad (3.20)$$

where  $J(\cdot)$  is defined on  $\Omega_R$ , i.e. on the fixed domain. This assumption is justified, in particular, when  $J(\cdot)$  is defined on or close to the boundary  $\Gamma$ . Let then  $p_0$  solve the adjoint problem

$$a_0(v, p_0; k) = -L_{(u_0;k)}(v), \quad \forall v \in V_R; \quad (3.21)$$

then the following asymptotic expansion holds

$$J(u_\epsilon; k) - J(u_0; k) = -\frac{2\pi}{\log \epsilon} \Re \frac{u_0^{\text{mean}}}{J_0(kR)} \frac{\overline{p_0^{\text{mean}}}}{J_0(kR)} + \dots, \quad (3.22)$$

where one has to notice that  $u_\Omega|_{\Omega_R} = u_0^R$  and  $p_\Omega|_{\Omega_R} = p_0^R$ . The topological gradient at  $x = x_0$  with respect to a ball is therefore given by

$$\mathcal{T}(x_0; k) = \Re \frac{u_0^{\text{mean}}}{J_0(kR)} \frac{\overline{p_0^{\text{mean}}}}{J_0(kR)}, \quad (3.23)$$

see Samet, Amstutz and Masmoudi (2003).

### 3.2. Helmholtz problem with Neumann condition in 2-d and 3-d

In a second example we consider the 2-d and 3-d Helmholtz problems similarly as discussed by Amstutz (2006) in the context of the modified Helmholtz equation, where no Dirichlet condition is used along  $\Gamma$  and where the problem formulation admits inclusions as well as holes with the additional freedom of having more general shapes of the inclusion and holes, respectively. The problem formulation is as follows

$$\begin{cases} \nabla \cdot (\alpha_\epsilon \nabla u_\epsilon) + \beta_\epsilon u_\epsilon = 0 & \text{in } \Omega \\ \frac{\partial}{\partial n} u_\epsilon - \Lambda u_\epsilon = h & \text{on } \Gamma. \end{cases} \quad (3.24)$$

Here,  $\Lambda \in \mathcal{L}(H^{\frac{1}{2}}(\Gamma), H^{-\frac{1}{2}}(\Gamma))$  is a boundary operator, e.g.  $\Lambda u_\epsilon = i\beta_\epsilon u_\epsilon$ , as in the last section, which is supposed to satisfy a dissipative condition

$$\Re \int_{\Gamma} (\Lambda \phi) \overline{\phi} d\gamma \leq 0 \quad \forall \phi \in H^{\frac{1}{2}}(\Gamma). \quad (3.25)$$

The coefficients in (3.24) are piecewise constant and satisfy

$$\alpha_\epsilon := \begin{cases} \alpha_0 & \text{if } x \in \Omega_\epsilon \\ \alpha_1 & \text{if } x \in B_\epsilon \end{cases}, \quad \beta_\epsilon := \begin{cases} \beta_0 & \text{if } x \in \Omega_\epsilon \\ \beta_1 & \text{if } x \in B_\epsilon. \end{cases} \quad (3.26)$$

Notice that now, the set  $B_\epsilon$  is not necessarily a ball of radius  $\epsilon > 0$  around  $x_0$  as in the last sections. There is a variety of cost functions that one may be interested in. Nevertheless, three of them seem to play a major role in the applications.

EXAMPLE 3.1 *We consider the examples of cost functions as follows.*

1. *The tracking cost functional as one of the most suitable ones for applications in this context. Here we have*

$$J(u_\epsilon; \alpha_\epsilon) := \int_{\Omega} \alpha_\epsilon |u_\epsilon - u_d|^2 dx$$

with  $u_d \in H^2(\Omega)$ . The linear operator  $L_u(u, \alpha_\epsilon)(v)$  obviously is

$$L_{(u, \alpha_\epsilon)}(v) = 2 \int_{\Omega} \alpha_\epsilon v \overline{(u - u_d)} dx, \quad \forall v \in H^1(\Omega).$$

In this case one has to take into account variations of  $J$  with respect to  $\alpha_\epsilon$ . Namely

$$\delta J := (\alpha_1 - \alpha_0) |B| |u - u_d|^2.$$

2. *A functional involving the gradients is given by*

$$J(u_\epsilon; \alpha_\epsilon) = \int_{\Omega} |\nabla(u_\epsilon - u_d)|^2 dx$$

with  $u_d \in H^3(\Omega)$ . Here the variations to be considered are given by

$$L_{(u, \alpha_\epsilon)}(v) = 2 \int_{\Omega} \alpha_\epsilon \nabla v \nabla \overline{(u - u_d)} dx$$

and

$$\delta J := (\alpha_1 - \alpha_0) \left\{ \nabla u(x_0)^T P \nabla \overline{u(x_0)} + |B| |\nabla(u(x_0) - u_d(x_0))|^2 \right\}$$

with a matrix  $P$  to be specified later (for a particular case).

3. *A functional concentrated on the boundary  $\Gamma$  is given by*

$$J(u_\epsilon) = \int_{\Gamma} |u_\epsilon - u_d|^2 ds$$

with  $u_d \in H^{3/2}(\Gamma)$ . Here, the variations to be considered are given by

$$L_{(u, \alpha_\epsilon)}(v) = 2 \int_{\Gamma} v \overline{(u - u_d)} ds \quad \text{and} \quad \delta J := 0.$$

In these cases, the topological derivative is analogous to the one derived by Amstutz (2006) in the context of the modified Helmholtz equation, namely:

EXAMPLE 3.2 *We give examples for inclusions first.*

1. *We first provide the results for a ball  $B := B_1(0)$  around  $x_0 = 0$*

$$\mathcal{T}(0; \alpha) = \Re \left\{ \frac{d\alpha_0(\alpha_1 - \alpha_0)}{(d-1)\alpha_0 + \alpha_1} |B| \nabla u(0) \overline{\nabla p(0)} - (\beta_1 - \beta_0) |B| u(0) \overline{p(0)} + \delta J \right\}. \quad (3.27)$$

*Notice that  $d = 2, 3$  is the dimensionality.*

2. *In the case of an ellipse with half-axis  $a, b$  one has in the 2-d case*

$$\mathcal{T}(0; \alpha) = \Re \left\{ (\alpha_1 - \alpha_0) \nabla u(0) P' \overline{\nabla p(0)} - (\beta_1 - \beta_0) \pi ab u(0) \overline{p(0)} + \delta J \right\}, \quad (3.28)$$

where the matrix  $P'$  is given by

$$P' = \pi ab \begin{pmatrix} \frac{\alpha_0(1+a) + \alpha_1(b-1)}{\alpha_0 a + \alpha_1 b} & 0 \\ 0 & \frac{\alpha_0(1+b) + \alpha_1(a-1)}{\alpha_0 b + \alpha_1 a} \end{pmatrix}. \quad (3.29)$$

## 4. Continuous dependence on frequencies

### 4.1. The 2-d Dirichlet case

The purpose of this section is to prove the continuity of the topological gradient  $\mathcal{T}(x; k)$  (3.23) with respect to the frequency parameter chosen in  $\mathcal{K} = \{k \in \mathbf{C} | \Im k \geq 0, J_0(kR) \neq 0\}$ .

LEMMA 4.1 *Let  $u_0^k, p_0^k$  be the solutions of*

$$\begin{cases} a_0(u, v; k) = \ell(v), \quad \forall v \in V \\ a_0(v, p; k) = -L_{(u_0; k)}(v), \quad \forall v \in V \end{cases} \quad (4.30)$$

for  $k \in \mathcal{K}$ , where  $a_0(u, v; k)$  is given by

$$a_0(u, v; k) = \int_{\Omega} \nabla u \nabla \bar{v} dx - k^2 \int_{\Omega} u \bar{v} dx - ik \int_{\Gamma_1} u \bar{v} d\gamma; \quad (4.31)$$

then the mappings

$$\begin{aligned} \mathcal{K} &\longrightarrow V \\ k &\longrightarrow u_0^k(\cdot), p_0^k(\cdot) \end{aligned} \quad (4.32)$$

are continuous.

PROOF We have, according to (4.31),

$$a_0(u, v; k) = a_0(u, v; 0) - k^2 \int_{\Omega} u \bar{v} dx - ik \int_{\Gamma_1} u \bar{v} d\gamma,$$

where

$$a_0(u, v; 0) = \int_{\Omega} \nabla u \nabla \bar{v} dx$$

is the classical form associated with the Laplacian. Therefore, we obviously have the standard ellipticity estimates

$$\begin{cases} c_0 \|u\|_{1,\Omega} \leq |u|_{1,\Omega} = a_0(u, u; 0) \\ a_0(u, v; 0) \leq C \|u\|_{1,\Omega} \|v\|_{1,\Omega}, \quad \forall u, v \in V. \end{cases} \quad (4.33)$$

Let a sequence  $\{k_n\}_{n \in \mathbf{N}} \subset \mathcal{K}$  be given such that  $k_n \rightarrow k$  as  $n \rightarrow \infty$ . Let  $u_n = u_0^{k_n} \in V$  be the associated solution, i.e.

$$a_0(u_n, v; 0) = k_n^2 \int_{\Omega} u_n \bar{v} dx + ik_n \int_{\Gamma_1} u_n \bar{v} d\gamma + \ell(v), \quad \forall v \in V \quad (4.34)$$

and let  $u_0^k$  solve

$$a_0(u_0^k, v; 0) = k^2 \int_{\Omega} u_0^k \bar{v} dx + ik \int_{\Gamma_1} u_0^k \bar{v} d\gamma + \ell(v), \quad \forall v \in V. \quad (4.35)$$

We first show that  $u_n$  is bounded. Indeed, otherwise  $\|u_n\|_{1,\Omega} \rightarrow \infty$  as  $n \rightarrow \infty$ . However, then  $z_n := \frac{u_n}{\|u_n\|_{1,\Omega}}$  is a sequence with  $\|z_n\|_{1,\Omega}$  within the Hilbert space  $V$ . Therefore, upon possibly choosing a subsequence, we have  $z_n \rightharpoonup z$  weakly in  $V$  with  $\|z\|_{1,\Omega} = 1$ . We divide (4.34) by  $\|u_n\|_{1,\Omega}$  and obtain

$$a_0(z_n, v; 0) = k_n^2 \int_{\Omega} z_n \bar{v} dx + ik_n \int_{\Gamma_1} z_n \bar{v} d\gamma + \frac{1}{\|u_n\|_{1,\Omega}} \ell(v), \quad \forall v \in V. \quad (4.36)$$

Because of  $z_n \rightharpoonup z$  in  $H^1(\Omega)$ , we may pass to the limit in (4.36) and obtain

$$a_0(z, v; 0) = k^2 \int_{\Omega} z \bar{v} dx + ik \int_{\Gamma_1} z \bar{v} d\gamma \quad \forall v \in V. \quad (4.37)$$

Since  $k \in \mathcal{K}$ , we conclude that  $z \equiv 0$ , in contradiction to  $\|z\|_{1,\Omega} = 1$ . Thus,  $\{u_n\}_{n \in \mathbf{N}}$  is a bounded sequence in  $V \subset H^1(\Omega)$ , and hence  $u_n \rightharpoonup u$  in  $V$ . By the compact embedding of  $V$  into  $H := L^2(\Omega)$  and into  $L^2(\Gamma)$ , we obtain

$$\begin{cases} u_n \rightharpoonup u & \text{in } V \\ u_n \xrightarrow{s} u & \text{in } L^2(\Omega) \\ u_n \xrightarrow{s} u & \text{in } L^2(\Gamma). \end{cases} \quad (4.38)$$

We show that  $u = u_0^k$ . Indeed, we may pass to the limit in

$$a_0(u_n, v; 0) = k_n^2 \int_{\Omega} u_n \bar{v} dx + ik_n \int_{\Gamma_1} u_n \bar{v} d\gamma + \ell(v), \quad \forall v \in V \quad (4.39)$$

in order to obtain

$$a_0(u, v; 0) = k^2 \int_{\Omega} u \bar{v} dx + ik \int_{\Gamma_1} u \bar{v} d\gamma + \ell(v), \quad \forall v \in V. \quad (4.40)$$

By the uniqueness of the solutions to (4.40), we conclude that  $u = u_0^k$ . Finally, we show that  $u_n \rightarrow u_0^k$  strongly in  $V$ . Indeed,

$$\begin{aligned} c_0 \|u_n - u_0^k\|_{1,\Omega} &\leq a_0(u_n - u_0^k, u_n - u_0^k; 0) \\ &\leq |k_n|^2 \int_{\Omega} |u_n - u_0^k|^2 dx + |(k_n^2 - k^2)| \left| \int_{\Omega} u_0^k \overline{(u_n - u_0^k)} dx \right| \\ &\quad + |k_n| \int_{\Gamma_1} |u_n - u_0^k|^2 d\gamma + |k_n - k| \left| \int_{\Gamma_1} u_0^k \overline{(u_n - u_0^k)} d\gamma \right|. \end{aligned} \quad (4.41)$$

Using the convergence properties (4.38) we conclude  $u_n \xrightarrow{s} u$  in  $V$ . As for the adjoint state, according to our assumptions on  $J(\cdot)$ , the mapping  $k \rightarrow L_{(u_0^k; k)}$  is continuous. We have

$$a_0(v, p_0^k; k) = -L_{(u_0^k; k)}(v), \quad \forall v \in V, k \in \mathcal{K}. \quad (4.42)$$

Certainly

$$\begin{cases} c_0 \|p_0^k\|_{1,\Omega} \leq |p_0^k|_{1,\Omega} = a_0(p_0^k, p_0^k; 0) \\ a_0(v, p_0^k; 0) \leq C \|p_0^k\|_{1,\Omega} \|v\|_{1,\Omega}, \quad \forall v \in V. \end{cases} \quad (4.43)$$

Let again  $\{k_n\}_{n \in \mathbb{N}} \subset \mathcal{K}$  be a sequence converging to a  $k \in \mathcal{K}$ , and let  $p_n := p_0^{k_n}$  be the associated solution to

$$a_0(v, p_n; 0) = k_n^2 \int_{\Omega} v \bar{p}_n dx + ik_n \int_{\Gamma_1} v \bar{p}_n d\gamma - J'(u_n; k)(v), \quad \forall v \in V. \quad (4.44)$$

As  $u_n \xrightarrow{s} u_0^k$  and  $L_{(u_n; k_n)} \rightarrow L_{(u_0^k; k)}$ , the same argument as in the first part of the proof applies to  $\{p_n\}$  and, hence, this sequence is bounded as well. Precisely the same arguments as above apply also for the passage to the limit. We obtain

$$a_0(v, p; 0) = k_n^2 \int_{\Omega} v \bar{p} dx + ik_n \int_{\Gamma_1} v \bar{p} d\gamma - L_{(u_0^k; k)}(v), \quad \forall v \in V.$$

However,

$$\begin{aligned}
c_0 \|p_n - p_0^k\|_{1,\Omega} &\leq a_0(p_n - p_0^k, p_n - p_0^k; 0) \\
&= a_0(p_n - p_0^k, p_n; 0) - a_0(p_n - p_0^k, p_0^k; k) \\
&= k_n^2 \int_{\Omega} (p_n - p_0^k) \overline{p_n} dx + ik_n \int_{\Gamma_1} (p_n - p_0^k) \overline{p_n} d\gamma \\
&\quad - k^2 \int_{\Omega} (p_n - p_0^k) \overline{p_0^k} dx - ik_n \int_{\Gamma_1} (p_n - p_0^k) \overline{p_0^k} d\gamma \\
&\quad - L_{(u_n; k_n)}(p_n - p_0^k) + L_{(u_0^k; k)}(p_n - p_0^k) \\
&= k_n^2 \int_{\Omega} (p_n - p_0^k) \overline{(p_n - p_0^k)} dx \\
&\quad + (k_n^2 - k^2) \int_{\Omega} (p_n - p_0^k) \overline{p_0^k} dx + i(k_n - k) \int_{\Gamma_1} (p_n - p_0^k) \overline{p_0^k} d\gamma \\
&\quad - (L_{(u_n; k)} - L_{(u_0^k; k)})(p_n - p_0^k) \longrightarrow 0.
\end{aligned} \tag{4.45}$$

This shows that  $p_n \rightarrow p_0^k$  and that the mapping  $k \rightarrow p_0^k$  is also continuous.  $\square$

REMARK 4.1 *The arguments in the proof of Lemma (4.1) can also be applied to show the continuity of the solutions  $u_0^k, p_0^k$  with respect to the right hand side  $h$ .*

THEOREM 4.1 *The topological gradient  $\mathcal{T}(x_0; k)$ , given by (3.23), is continuous with respect to the parameter  $k$  and the right hand side  $h$ .*

PROOF The statement is now obvious from the continuity of the functions  $u_0^k, p_0^k$  and the representation of the topological gradient in (3.23).  $\square$

## 4.2. The 2-D and 3-D Neumann case

We now briefly discuss the topological gradients (3.27), (3.28) for the 2-d and 3-d problem (3.24). The difference with the analysis of the problem (3.6) lies in the appearance of the parameter  $\alpha_0$  in the problem on the entire unperturbed domain, and, if considered, the possible generality of the operator  $\Lambda$ . Moreover, according to the Neumann conditions everywhere, the reference space in Lemma 4.1 has to be adjusted for the case under consideration, i.e. one has to work in the space

$$V_0 := \{u \in H^1(\Omega) \mid \int_{\Omega} u dx = 0\}.$$

In addition, as  $\Lambda$  satisfies the dissipativity inequality (3.25), variations in  $\Lambda$  can be treated in the same way as those handled in Lemma 4.1. It is further

obvious that the solution of the problem without any perturbation does not depend on the parameters  $\beta_1, a, b$ . Therefore, the only dependence that has to be taken into account in addition to Lemma 4.1 is the dependence of  $u_0, p_0$  on the parameter  $\alpha_0$ . To include this into Lemma 4.1 is an easy exercise. Indeed, in Hlaváček et al. (2009), where the Lamé system is investigated with respect to variations in the coefficients, such a parameter dependence has been discussed for a more complex problem. Thus, we may archive these arguments in the following

**THEOREM 4.2** *The topological gradients (3.27) and (3.28) are continuous with respect to the parameters  $\alpha_0, \alpha_1, \beta_0, \beta_1, a, b$ .*

**REMARK 4.2** *Notice that  $b$  may be taken equal to zero, to the effect that the hole degenerates to a straight crack.*

## 5. The concept of robustness for the topological derivative with respect to variations in frequency and system parameters

In the paper of Hlaváček et al. (2009), the authors introduced two notions for the robustness of topological derivatives with respect to changes in system parameters, in fact, the Lamé moduli given in elastostatics. We adjust the definition given in Hlaváček et al. (2009) for the situation discussed in this paper.

**DEFINITION 5.1** *Let us consider the topological derivative  $x \rightarrow \mathcal{T}(x; (k, P))$ , with the parameter set  $P \in \mathcal{P}$  replaced by the boundary data*

$$h \in \mathcal{H} = \{h \mid \|h\|_{H^{\frac{1}{2}}(\Gamma_1)^*}\}.$$

*We say that we have a worst-case scenario, if*

$$(k^*, h^*) = \arg \max_{(k, h) \in \mathcal{K} \times \mathcal{H}} \mathcal{T}(x; (k, h)). \quad (5.46)$$

*We say that we have a maximum-range scenario, if*

$$(k^\#, h^\#) = \arg \min_{(k, h) \in \mathcal{K} \times \mathcal{H}} \mathcal{T}(x; (k, h)). \quad (5.47)$$

We are thus looking for the upper and lower bounds of the topological derivative with respect to the frequency range and the data. The obvious result now is as follows.

**THEOREM 5.1** *Problems (5.46) and (5.47) have at least one solution.*

**PROOF** For the proof we notice that the set  $\mathcal{K} \times \mathcal{H}$  is compact, which, together with the continuity of the topological gradient, gives the result.  $\square$

## 6. Imaging of small scatters from boundary measurements

### 6.1. The setting

We consider the problem of reconstructing a set of small scatters from boundary measurements. The shape functional to be minimized is defined as

$$J(u^1, u^2, \dots, u^M) = \sum_{m=1}^M \int_{\Gamma} |u^m - u_d^m|^2 ds, \quad (6.48)$$

where  $m$  represents the  $m$ -th measurement and  $M$  is the total number of measurements. In addition,  $u_d^m$  is the boundary measurement, computed from the model problem. More precisely, we consider a set of small scatter with contrast  $\gamma$  on the coefficient of the main part of the operator. Finally,  $u_m$  is a solution to the forward problem of the form:

$$\begin{cases} \Delta u^m + k^2 u^m = 0 & \text{in } \Omega \\ \frac{\partial}{\partial n} u^m - i k u^m = h^m & \text{on } \Gamma, \end{cases} \quad (6.49)$$

where  $k$  is the wave number and  $h^m$  is the boundary data used to produce the  $m$ -th boundary measurement  $u_d^m$ . The topological derivative of  $J(u^1, u^2, \dots, u^M)$  with respect to the nucleation of a small circular inclusion is given by the sum

$$\mathcal{T}(x) = -2\pi \frac{1-\gamma}{1+\gamma} \sum_{m=1}^M \Re\{\nabla u^m(x) \nabla \overline{p^m(x)}\}, \quad (6.50)$$

where  $p^m$  is a solution to the adjoint equation, associated with the  $m$ -th measurement, that is

$$\begin{cases} \Delta p^m + k^2 p^m = 0 & \text{in } \Omega \\ \frac{\partial}{\partial n} p^m + i k p^m = -2(u^m - u_d^m) & \text{on } \Gamma. \end{cases} \quad (6.51)$$

The basic idea consists in plotting the topological derivative field  $\mathcal{T}(x)$  according to (6.50). It is expected that the more  $\mathcal{T}(x)$  is negative, the more likely  $x$  is within the hidden scatter we are looking for. The measurements are obtained by setting  $h^m$  as

$$h^m = \exp(-ik(x_1 \cos \theta_m + x_2 \sin \theta_m)), \quad \text{with } \theta_m = \frac{m-1}{M} \pi, \quad (6.52)$$

where  $x = (x_1, x_2)$ . In particular, we set  $M = 32$  and the contrast  $\gamma = 0.1$ . The domain  $\Omega$  is given by a unit disk with center at the origin. The boundary value problems are solved with the standard Finite Element Method. We consider two representative examples. For a comprehensive set of numerical experiments in the context of imaging of small scatters, see the series of two papers by Le Louër and Rapún (2022a,b).



### Example 1

In this first example, the target is given by one scatter of radius 0.1 and center at  $(0.5, 0.3)$ , as shown in Fig. 1. We set varying working frequency  $k$ , namely 4, 8, 16 and 32. The obtained results are presented in Fig. 2. From an analysis of this figure, we observe that the hidden scatter is highlighted by the topological derivative field. However, the higher is the frequency, the better is the resolution of the imaging.

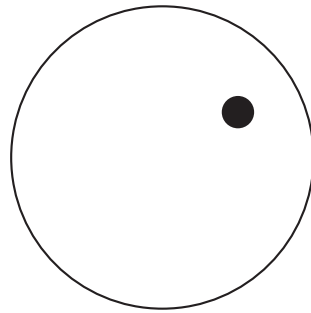


Figure 1. Example 1. Target to be reconstructed

### Example 2

In this example, we consider the target given by three scatters of radius 0.05 and centers at  $(0.5, 0.3)$ ,  $(0.0, -0.4)$  and  $(-0.3, 0.2)$ , as shown in Fig. 3(a). The working frequency is now set as  $k = 32$ . The obtained result is presented in Fig. 3(b), where we observe that the three hidden scatters are clearly highlighted by the topological derivative field, as expected.

Finally, in order to confirm the robustness of the topological derivative in the context of imaging of small scatters, we consider uncertainty on the working frequency  $k$ . More precisely, the boundary measurements  $u_d^m$  are computed after replacing  $k$  by  $\tilde{k}^m$ , for  $m = 1, \dots, M$ , where each working frequency  $\tilde{k}^m$  is corrupted with White Gaussian Noise (WGN). In contrast,  $u^m$  and  $p^m$  are computed by considering uncorrupted frequency  $k$ . The obtained topological derivative fields  $\mathcal{T}(x)$  for 2%, 4%, 8% and 16% of WGN are presented in Fig. 4. From an analysis of these figures, we observe that the three scatters can be identified even in the presence of noise. Even if, for 16% of noise, the result is rather degraded, nevertheless it is still possible to identify the three scatters.

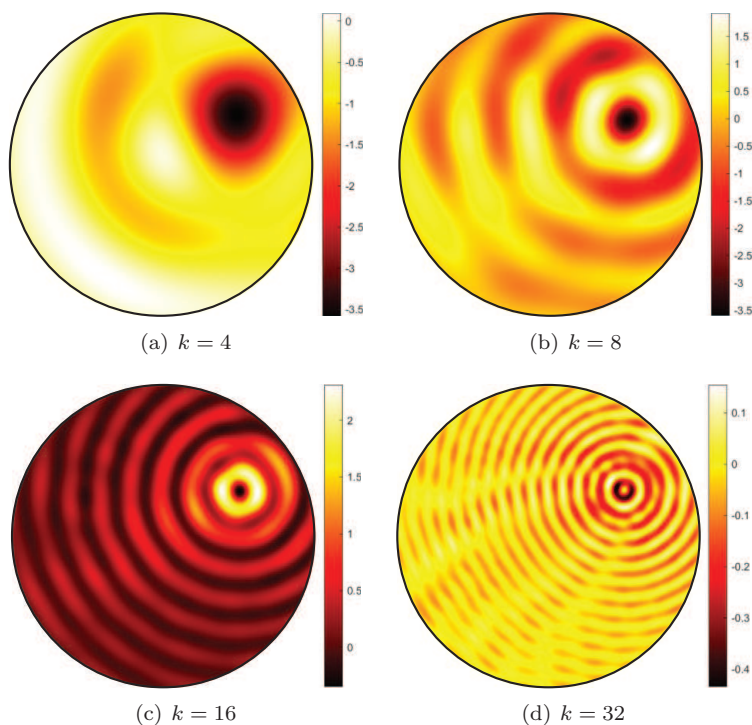


Figure 2. Example 1. Topological derivative fields for varying working frequencies

## References

- ALLAIRE, G., JOUVE, F. AND TOADER, A. M. (2004) Structural optimization using sensitivity analysis and a level-set method. *Journal of Computational Physics*, **194**(1): 363–393.
- AMSTUTZ, S. (2006) Sensitivity analysis with respect to a local perturbation of the material property. *Asymptotic Analysis*, **49**(1-2): 87–108.
- AMSTUTZ, S. (2022) An introduction to the topological derivative. *Engineering Computations*, **39**(1): 3–33.
- AMSTUTZ, S. AND NOVOTNY, A. A. (2010) Topological optimization of structures subject to von Mises stress constraints. *Structural and Multidisciplinary Optimization*, **41**(3): 407–420.
- ASSOUS, F., CIARLET, P. AND LABRUNIE, S. (2018) *Mathematical Foundations of Computational Electromagnetism. Applied Mathematical Sciences*. Springer Nature Switzerland.
- BARROS, G., FILHO, J., NUNES, L. AND XAVIER, M. (2022) Experimental validation of a topological derivative-based crack growth control method

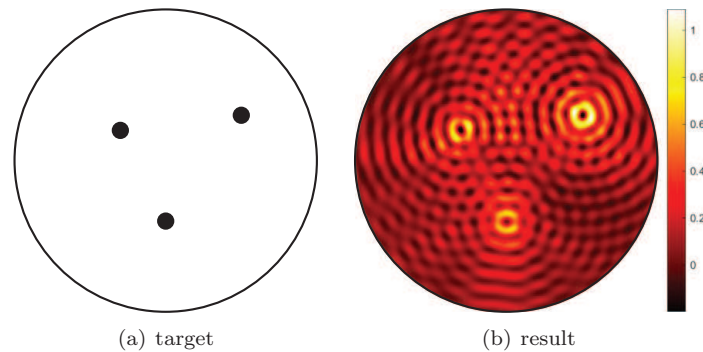


Figure 3. Example 2. Target to be reconstructed on the left (a) and topological derivative field on the right (b)

- using digital image correlation. *Engineering Computations*, **39**(1): 438–454.
- BAUMANN, PH. AND STURM, K. (2022) Adjoint-based methods to compute higher-order topological derivatives with an application to elasticity. *Engineering Computations*, **39**(1): 60–114.
- BONNET, M. (2022) On the justification of topological derivative for wave-based qualitative imaging of finite-sized defects in bounded media. *Engineering Computations*, **39**(1): 313–336.
- BONNET, M. AND GUZINA, B. B. (2004) Sounding of finite solid bodies by way of topological derivative. *International Journal for Numerical Methods in Engineering*, **61**(13): 2344–2373.
- CANELAS, A. AND ROCHE, J.R. (2022) Shape and topology optimal design problems in electromagnetic casting. *Engineering Computations*, **39**(1): 147–171.
- DELFOUR, M.C. (2022) Topological derivatives via one-sided derivative of parametrized minima and minimax. *Engineering Computations*, **39**(1): 34–59.
- FERNANDEZ, L. AND PRAKASH, R. (2022) Imaging of small penetrable obstacles based on the topological derivative method. *Engineering Computations*, **39**(1): 201–231.
- FERRER, A. AND GIUSTI, S.M. (2022) Inverse homogenization using the topological derivative. *Engineering Computations*, **39**(1): 337–353.
- GARREAU, S., GUILLAUME, PH. AND MASMOUDI, M. (2001) The topological asymptotic for PDE systems: the elasticity case. *SIAM Journal on Control and Optimization*, **39**(6): 1756–1778.
- GUZINA, B. B. AND CHIKICHEV, I. (2007) From imaging to material identification: a generalized concept of topological sensitivity. *Journal of the Mechanics and Physics of Solids*, **55**(2): 245–279.

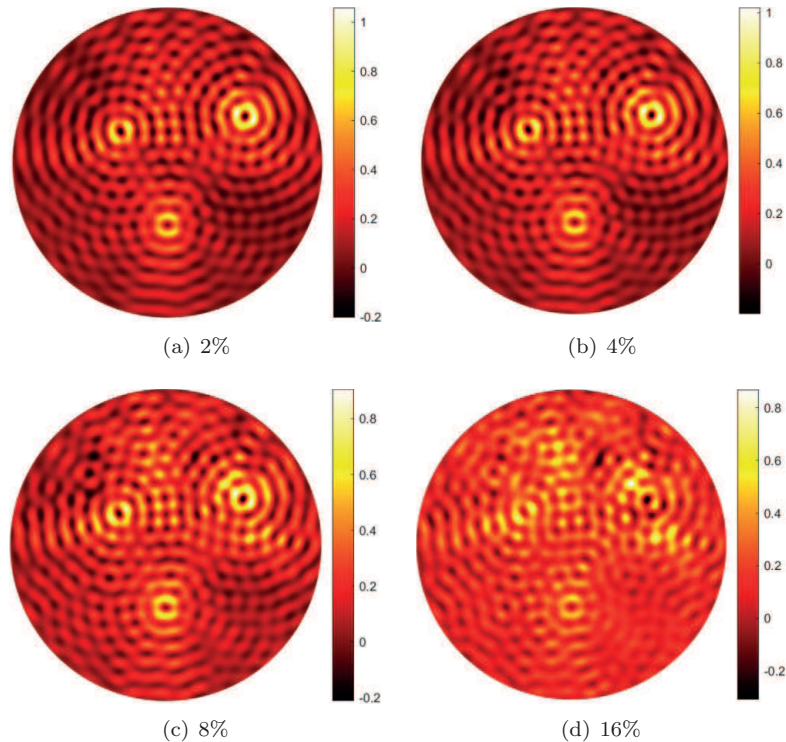


Figure 4. Example 2. Topological derivative fields for varying levels of WGN

- HENROT, A. AND PIERRE, M. (2005) *Variation et optimisation de formes. Mathématiques et applications*, **48**, Springer-Verlag, Heidelberg.
- HINTERMÜLLER, M. (2005) Fast level set based algorithms using shape and topological sensitivity. *Control and Cybernetics*, **34**(1): 305–324.
- HLÁVÁČEK, I., NOVOTNY, A. A., SOKOŁOWSKI, J. AND ŽOCHOWSKI, A. (2009) On topological derivatives for elastic solids with uncertain input data. *Journal of Optimization Theory and Applications*, **141**(3): 569–595.
- ILIN, A. M. (1992) *Matching of Asymptotic Expansions of Solutions of Boundary Value Problems. Translations of Mathematical Monographs*. American Mathematical Society, **102**, Providence, RI. Translated from Russian by V. V. Minachin.
- KLEWE, PH., LAURAIN, A. AND SCHMIDT, K. (2022) Shape optimization in acoustic-structure interaction. *Engineering Computations*, **39**(1): 172–200.
- LE LOUËR, F. AND RAPÚN, M.L. (2022a) Topological sensitivity analysis re-

- visited for timeharmonic wave scattering problems. Part I: The free space case. *Engineering Computations*, **39**(1):232–271.
- LE LOUËR, F. AND RAPÚN, M.L. (2022b) Topological sensitivity analysis revisited for timeharmonic wave scattering problems. Part II: Recursive computations by the boundary integral equation method. *Engineering Computations*, **39**(1):272–312.
- MASMOUDI, M., POMMIER, J. AND SAMET, B. (2005) The topological asymptotic expansion for the Maxwell equations and some applications. *Inverse Problems*, **21**(2):547–564.
- NOVOTNY, A. A. AND SOKOŁOWSKI, J. (2013) *Topological Derivatives in Shape Optimization. Interaction of Mechanics and Mathematics*. Springer-Verlag, Berlin, Heidelberg.
- NOVOTNY, A. A. AND SOKOŁOWSKI, J. (2020) *An Introduction to the Topological Derivative Method. Springer Briefs in Mathematics*. Springer Nature Switzerland.
- NOVOTNY, A. A., SOKOŁOWSKI, J. AND ŻOCHOWSKI, A. (2019) *Applications of the Topological Derivative Method. Studies in Systems, Decision and Control*. Springer Nature Switzerland.
- NOVOTNY, A. A., GIUSTI, S.M. AND AMSTUTZ, S. (2022) Guest Editorial: On the topological derivative method and its applications in computational engineering. *Engineering Computations*, **39**(1):1–2.
- RAKOTONDRAINIBE, L., ALLAIRE, G. AND ORVAL, P. (2022) Topological sensitivity analysis with respect to a small idealized bolt. *Engineering Computations*, **39**(1):115–146.
- ROMERO, A. (2022) Optimum design of two-material bending plate compliant devices. *Engineering Computations*, **39**(1):395–420.
- SAMET, B., AMSTUTZ, S. AND MASMOUDI, M. (2003) The topological asymptotic for the Helmholtz equation. *SIAM Journal on Control and Optimization*, **42**(5): 1523–1544.
- SANTOS, R.B. AND LOPES, C.G. (2022) Topology optimization of structures subject to selfweight loading under stress constraints. *Engineering Computations*, **39**(1): 380–394.
- SCHUMACHER, A. (1995) *Topologieoptimierung von bauteilstrukturen unter verwendung von lochpositionierungskriterien*. Ph.D. Thesis, Universität-Gesamthochschule-Siegen, Siegen - Germany.
- SOKOŁOWSKI, J. AND ŻOCHOWSKI, A. (1999a) On the topological derivative in shape optimization. *SIAM Journal on Control and Optimization*, **37**(4): 1251–1272.
- SOKOŁOWSKI, J. AND ŻOCHOWSKI, A. (1999b) Topological derivatives for elliptic problems. *Inverse Problems*, **15**(1): 123–134.
- SOKOŁOWSKI, J. AND ŻOCHOWSKI, A. (2001) Topological derivatives of shape functionals for elasticity systems. *Mechanics of Structures and Machines*, **29**(3): 333–351.
- SOKOŁOWSKI, J. AND ZOLÉSIO, J. P. (1992) *Introduction to Shape Optimization - Shape Sensitivity Analysis*. Springer-Verlag, Berlin, Germany.

- XAVIER, M. AND VAN GOETHEM, N. (2022) Brittle fracture on plates governed by topological derivatives. *Engineering Computations*, **39**(1): 421–437.
- YERA, R., FORZANI, L., MÉNDEZ, C.G. AND HUESPE, A.E. (2022) A topology optimization algorithm based on topological derivative and level-set function for designing phononic crystals. *Engineering Computations*, **39**(1): 354–379.